Presented at The 1989 Particle Accelerator Conference
Hyatt Regency Hotel, Chicago, IL
March 20-23, 1989

Measurement of the Magnetic Field Coefficients of Particle Accelerator Magnets *

J. Herrera, G. Ganetis, R. Hogue, E. Rogers, P. Wanderer, and E. Willen

Brookhaven National Laboratory
Upton, New York 11973

I. Introduction

An important aspect in the development of magnets to be used in particle accelerators is the measurement of the magnetic field in the beam aperture. In general it is necessary to measure the harmonic multipoles in the dipole, quadrupole, and sextupole magnets for a series of stationary currents (plateaus). This is the case for the Superconducting Super Collider (SSC) which will be ramped to high field over a long period (~ 1000 sec.) and then remain on the flat top for the duration of the particle collision phase. In contrast to this mode of operation, the Booster ring being constructed for the Brookhaven AGS, will have a fast ramp rate of approximately 10 Hz. The multipole fields for these Booster magnets must therefore be determined "on the ramp". In this way the effect of eddy currents will be taken into account.

The measurement system which we will describe in this paper is an outgrowth of that used for the SSC dipoles. It has the capability of measuring the field multipoles on both a plateau or during a fast ramp. In addition, the same basic coil assembly is used to obtain the magnetic multipoles in dipole, quadrupole, and sextupole magnets.

II Multipole Fields and Voltages

For a general accelerator-type magnet, the magnetic field in its aperture is best described by the two dimensional cylindrical representation

$$\vec{B}(r,\theta) = \sum_{n=1} C(n)\left(\frac{r}{R}\right)^{n-1} \times \left[\vec{I}_r \sin n(\theta-\alpha_n) + \vec{I}_\theta \cos n(\theta-\alpha_n)\right] \qquad (1)$$

where $C(n)$ is the amplitude (tesla) of the nth multipole at a reference radius R, while α_n is the angular orientation of the multipole with a value in the range: $0 \le \alpha_n < 2\pi/n$. As discussed previously[1,2], this representation is applicable to any magnet, whatever its dominant multipole, and is particularly useful when finding the voltage induced in a winding rotating in the magnetic field. Figure 1 shows a cross sectional view of the coil with its five windings: two dipole bucking windings designated as 1 and 2, two quadrupole bucking windings (4 and 5) and a tangential winding (3). The angle ($2\epsilon_D$) between the two dipole bucking windings has been chosen such that when these windings are connected in series with the tangential winding, the net voltage due to the dipole component of field is zero. Similarly, the voltages in the two quadrupole windings buck out the quadrupole voltage component appearing in the tangential winding. To be more specific, the voltages induced in the three sets of windings, when rotating clockwise at a constant angular velocity (ω) in a magnetic field given by Eq.(1), are

$$v_D = -\sum_{n=1} C(n)\left(\frac{r_c}{R}\right)^{n-1} 4\ell r_c N_D \omega \sin\frac{n\pi}{2} \times \cos n\epsilon_D \cos n(\omega t - \delta_D + \alpha_n) \ , \qquad (2)$$

$$v_Q = -\sum_{n=1} C(n)\left(\frac{r_c}{R}\right)^{n-1} 4\ell r_c N_Q \omega \sin\frac{n\pi}{4} \times \left[1+(-1)^n\right]\cos(n\eta_Q)\cos n(\omega t - \delta_Q + \alpha_n) \ , \qquad (3)$$

and

$$v_3 = -\sum_{n=1} C(n)\left(\frac{r_c}{R}\right)^{n-1} \times 2\ell r_c N_3 \omega \sin\frac{n\Delta}{2}\cos n(\omega t - \delta_3 + \alpha_n) \ . \qquad (4)$$

Here the axial length of all the windings is ℓ, while the three angles (δ_D, δ_Q, δ_3) are initial angular positions. The other symbols, as well as their numerical values, are presented in Table 1. Consistent with these equations, the condition for dipole field bucking is

$$N_3 \sin\frac{\Delta}{2} - 2N_D \cos\epsilon_D = 0 \ , \qquad (5)$$

and that for the quadrupole is

$$N_3 \sin\Delta - 4N_Q \cos 2\eta_Q = 0 \ . \qquad (6)$$

When the coil assembly is held in a fixed angular position (θ_p) and the magnet current is ramped, such that the three windings see a changing magnetic flux, then the instantaneous voltages are

$$v_D = -\sum_{n=1}\left(\frac{r_c}{R}\right)^{n-1}\frac{4\ell r_c N_D}{n}\sin\frac{n\pi}{2}\cos n\epsilon_D \times \left\{\dot{R}_n(t)\sin n(\theta_p-\delta_D) + \dot{S}_n(t)\cos n(\theta_p-\delta_D)\right\} \ . \qquad (7)$$

$$v_Q = -\sum_{n=1}\left(\frac{r_c}{R}\right)^{n-1}\frac{4\ell r_c N_Q}{n}\sin\frac{n\pi}{4}\left[1+(-1)^n\right]\cos n\eta_Q \times \left\{\dot{R}_n(t)\sin n(\theta_p-\delta_Q) + \dot{S}_n(t)\cos n(\theta_p-\delta_Q)\right\} \ . \qquad (8)$$

$$v_3 = -\sum_{n=1}\left(\frac{r_c}{R}\right)^{n-1}\frac{2\ell r_c N_3}{n}\sin\frac{n\Delta}{2} \times \left\{\dot{R}_n(t)\sin n(\theta_p-\delta_3) + \dot{S}_n(t)\cos n(\theta_p-\delta_3)\right\} \ . \qquad (9)$$

The time dependence in these equations appears through what we call the multipole harmonic rate functions, $\dot{R}_n(t)$ and $\dot{S}_n(t)$, which are defined as

$$\dot{R}_n(t) = \frac{d}{dt}(C(n)\cos n\alpha_n) \ , \qquad (10)$$

$$\dot{S}_n(t) = \frac{d}{dt}(C(n)\sin n\alpha_n) \ . \qquad (11)$$

* Work performed under the auspices of the U.S. Department of energy.

As the magnetic field varies with time, not only does the amplitude of the multipole (C_n) change but also the associated multipole angular orientation (α_n), and the harmonic rate functions express their combined effect. As can be readily verified, the bucking conditions for the ramping field case are again given by Eqs. (5) and (6).

III. Multipole Measurements on a Current Plateau

In Fig. (2) we show the block diagram for the overall measurement system. When determining the magnetic multipoles at a fixed magnet current, the procedure is similar to that described in Refs. 1 and 2. However, since we are now using analogue instead of digital bucking, the net bucked voltage is derived directly from the three windings connected in series giving the bucked voltage

$$v_B = v_3 - v_D - v_Q \qquad (12)$$

Thus it is the three voltages v_D, v_Q, and v_B that are read digitally at 64 equally spaced points over one shaft rotation of the coil assembly. The angular encoder supplies the appropriate timing pulses. A Fourier analysis (FFT) of the voltages v_D and v_Q and a comparison with Eqs. (1) and (2), yield the dipole $(C(1), \alpha_1)$ and quadrupole $(C(2), \alpha_2)$ multipole components of the field. Similarly, a Fourier analysis of the bucked voltage (v_B) allows one to calculate the higher multipoles ($n = 3, \ldots 11$).

IV. Multipole Measurements during a Current Ramp

In this case the basic electrical system remains unchanged from that depicted in Fig. 2. However as might be expected by considering Eqs. (7) through (12), the induced voltages in the windings are now determined primarily by the harmonic rate functions, and it is these functions which must first be found from the voltage measurements. A flow chart showing the various analytical steps that are carried through in arriving at the multipoles $(\hat{C}(n), \hat{\alpha}_n)$ is presented in Fig. (3). (We use "hatted symbols" to emphasise that these multipole coefficients are the changes from some initial values.) For each of 64 angular positions (k = 0, 1, ..., 63) of the measuring coil, the magnet current is ramped and observations taken for the three voltages and the ramping current at 49 discrete times (j = 0, ..., 48) during the ramp. Since all the current ramps (I vs. t) will not be identical, a least square fit (each set of five currents fitted to a quadratic function of time) is made and the currents $I(k,j)$ as well as the instantaneous slopes s(k,j) are determined. The calculated slopes are now used to correct the instantaneous voltages measured by the three windings. At a given average current a Fourier analysis of the angular dependence of the voltage is performed, yielding (on comparison with Eqs. (7), (8), and (12)) the harmonic rate functions. It is the integrals of these functions which are directly related to the magnetic multipoles $(\hat{C}(n), \hat{\alpha}_n)$ (see Eqs. (10) and (11)).

References

1) J. Herrera, H. Kirk, A. Prodell, and E. Willen, Proc. of the 12th International Conference on High Energy Accelerators, Fermilab (1983).

2) E. Willen, P. Dahl, J. Herrera, AIP Conference Proc. 153. Summer School on Particle Accelerators (1984 & 1985), Vol.2, p1228.

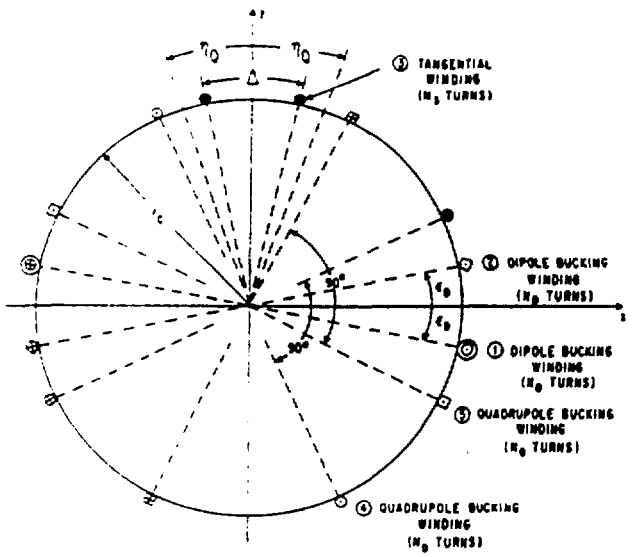

Fig. 1: Cross sectional view of the coil, showing the angular distribution of the multipole windings.

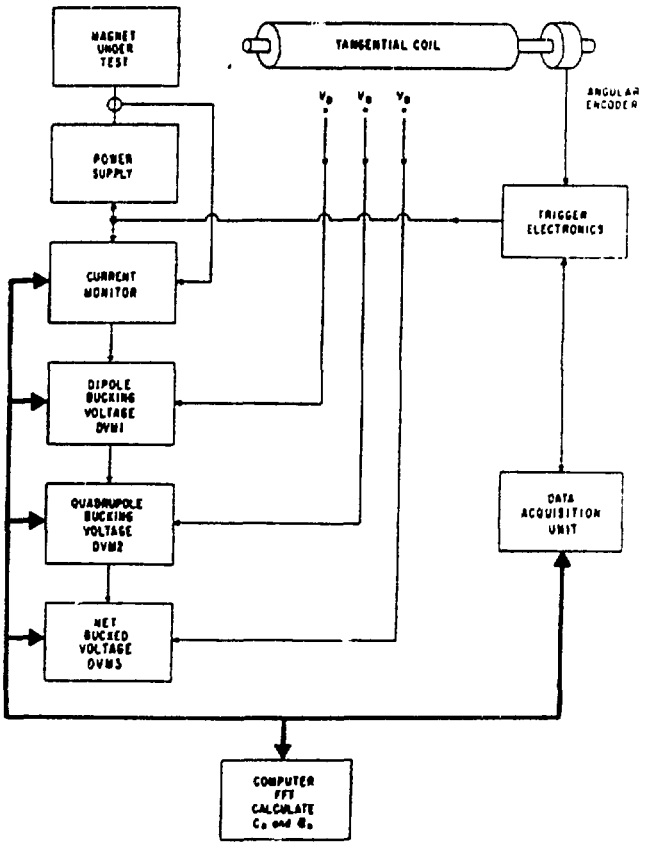

Fig. 2: Block diagram of electrical system for tangential coil measurements with analogue bucking.

PROPERTY	SYMBOL	VALUE
Length of all windings	ℓ	36.5"
Radial position of all windings	r_c	0.8660"
Turns of tangential winding (TW)	N_3	20
Turns of dipole bucking winding (DBW)	N_D	3
Turns of quadrupole bucking winding (QBW)	N_Q	3
Angular width of tangential winding	Δ	25.7143°
Angle for dipole bucking	ϵ_D	42.1205°
Angle for quadrupole bucking	η_Q	21.8428°

Table 1: Physical Characteristic of the Three Windings.

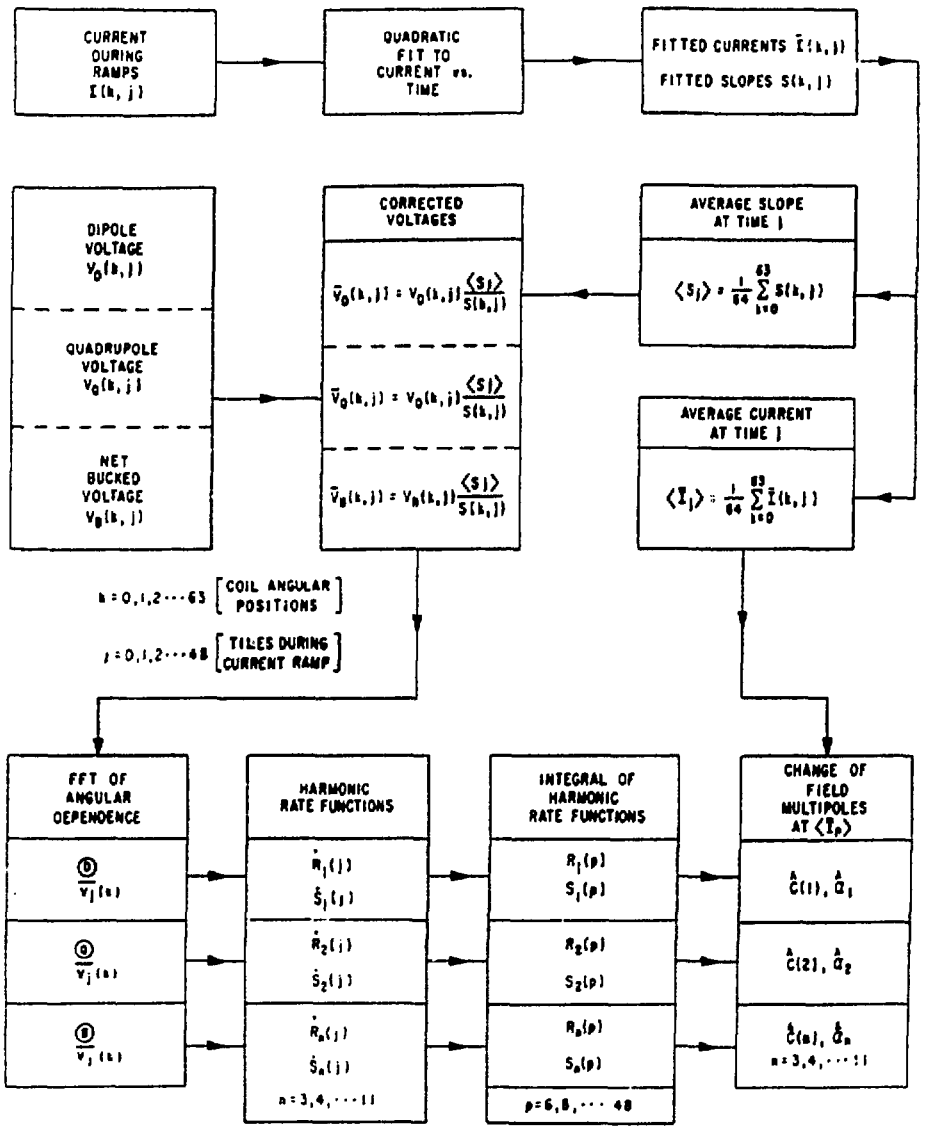

Fig. 3: Flow chart for obtaining the multipole components for a ramping field. The measuring coil angular positions are characterized by the index k, while the times during the ramps have the index j.

DISCLAIMER